Journal of Engineering and Applied Sciences 13 (24): 10474-10481, 2018
ISSN: 1816-949X

MHD Stagnation-Point Flow of a Nanofluid past a Stretching/Shrinking Sheet with Induced Magnetic Field

[1]Mohamad Mustaqim Junoh, [1, 2]Fadzilah Md Ali and [3]Ioan Pop
[1] Department of Mathematics, Universiti Putra Malaysia (UPM), 43400 Serdang, Selangor, Malaysia
[2]Department of Mathematics & Institute for Mathematical Research,
Universiti Putra Malaysia, 43400 UPM Serdang, Selangor, Malaysia
[3]Department of Mathematics, Babes-Bolyai University, R-400084 Cluj-Napoca, Romania

Abstract: The problem of the steady two dimensional stagnation-point flow of an incompressible electrically conducting nanofluid caused by a stretching/shrinking surface is studied. The effect of an induced magnetic field is taken into account. The nonlinear partial differential equations are transformed into nonlinear ordinary differential equations via. similarity transformations. The transformed governing equations are solved numerically using the shooting method which built-in function in Maple Software. The effects of governing parameters on the skin friction coefficient, the local Nusselt number, the local sherwood number and the velocity, temperature and concentration profiles are also presented in this study. It is found that dual solutions exist for the shrinking case. Therefore, a stability analysis is performed to verify which solution is stable and it is found that the first solution is physically stable while the second solution is unstable.

Key words: Dual solutions, induced magnetic field, nanofluid, stagnation-point, stretching/shrinking, verify

INTRODUCTION

The theory of nanofluid was first introduced by Choi (1995) where it refers to the dilution of nanometer-sized particles (= 100 nm) in a fluid. Nanofluid gains many attractions from researchers these days because of their extremely good in improving thermal conductivity property (Ishak *et al*., 2006). Recently, the study of convective heat transfer in nanofluid becomes an active research area due to its heat transfer enhancements characteristics. The fact that cooling is one of the technical challenges faced by many industries including microelectronic, transportation, solid-state lighting and manufacturing is the reason why the idea of nanofluid has been proposed. Choi (1995) has conducted the pioneering experimental research on thermal conductivity enhancement of nanofluid. The result showed that a very small amount of nanoparticles would double increase the thermal conductivity of the fluid. Due to this interesting characteristic, many investigators studied the nanofluid flow both theoretically and experimentally.

Later, Kuznetsov and Nield (2010) studied analytically the natural convective boundary layer flow of nanofluid past a vertical plate. They extended the study of the Pohlhausen-Kuiken-Bejan problem to the case of nanofluid using the model of Buongiorno (2006). Mustafa *et al.* (2011) solved analytically the problem of nanofluid near a stagnation-point towards a stretching surface using homotopy analysis method. Later, Bachok *et al.* (2011) studied the stagnation-point flow over a stretching/shrinking sheet in a nanofluid and found that for the shrinking case the solution is non-unique (dual solutions). Zaimi *et al.* (2012) solved numerically using a shooting method the problem of a steady two-dimensional boundary layer flow and heat transfer past a permeable shrinking sheet in a nanofluid with thermal radiation and suction effects. Their results also show that dual solutions exist in a certain range of suction parameter. The study of the stretching/shrinking sheet problems under various physical conditions have been studied by several authors such as Nandy and Mahapatra (2013), Aman *et al.* (2013), Makinde *et al.* (2013) and Mansur *et al.* (2015). Little works have been done on the problem of boundary layer flow with the effect of the induced magnetic field, namely, Kumari *et al.* (1990), Takhar *et al.* (1993) and Ali *et al.* (2011a-c). Therefore with the above motivations, the present study is to study the problem of a stagnation-point flow of an incompressible electrically conducting nanofluid towards a stretching/shrinking surface in the presence of induced magnetic field.

Corresponding Author: Fadzilah Md Ali, Department of Mathematics, Universiti Putra Malaysia (UPM), 43400 Serdang, Selangor, Malaysia

MATERIALS AND METHODS

Mathematical formulation: We consider a steady two dimensional stagnation-point flow of an incompressible electrically conducting nanofluid caused by a stretching/shrinking surface with the effect of the induced magnetic field. The coordinate system is selected in which axis is in horizontal direction and axis is in vertical direction. At the plate (y = 0), the temperature and the concentration take a constant value T_w and C_w, respectively. The ambient values as for temperature and concentration are T_8 and C_8, respectively.

According to the boundary layer approximation (Davies, 1963; Kuznetsov and Nield, 2010), the governing equations related to the problem can be written as:

$$\frac{\partial u}{\partial x}+\frac{\partial v}{\partial y}=0 \tag{1}$$

$$\frac{\partial H_1}{\partial x}+\frac{\partial H_2}{\partial y}=0 \tag{2}$$

$$u\frac{\partial u}{\partial x}+v\frac{\partial u}{\partial y}-\frac{\mu_m}{4\pi\rho_f}\left(H_1\frac{\partial H_1}{\partial x}+H_2\frac{\partial H_2}{\partial y}\right)=\left(u_e\frac{\partial u_e}{\partial x}-\frac{\mu_m H_e}{4\pi\rho_f}\frac{\partial H_e}{\partial x}\right)+\nu\frac{\partial^2 u}{\partial y^2} \tag{3}$$

$$u\frac{\partial H_1}{\partial x}+v\frac{\partial H_1}{\partial y}-H_1\frac{\partial \mu}{4\pi\rho_f}H_2\frac{\partial \mu}{\partial x}=\xi\frac{\partial^2 H_2}{\partial y^2} \tag{4}$$

$$u\frac{\partial T}{\partial x}+v\frac{\partial T}{\partial y}=\alpha\frac{\partial^2 T}{\partial y^2}+\varepsilon D_B\frac{\partial T}{\partial y}\frac{\partial C}{\partial y}+\varepsilon\left(\frac{D_T}{T_\infty}\right)\left(\frac{\partial T}{\partial y}\right)^2 \tag{5}$$

$$u\frac{\partial C}{\partial x}+v\frac{\partial C}{\partial y}=D_B\frac{\partial^2 C}{\partial y^2}+\left(\frac{D_T}{T_\infty}\right)\frac{\partial^2 T}{\partial y^2} \tag{6}$$

Where:

u and v = The velocity components along the x and axes

v = The kinematic viscosity of the fluid

$\varepsilon=\frac{(\rho c)_p}{(\rho c)_f}$ = The ratio of nanoparticle heat capacity to the base fluid heat capacity $\alpha=\frac{k}{\rho c_p}$

Where:

k = The thermal conductivity

$\xi=\frac{1}{4\pi\sigma}$ = The magnetic diffusivity

σ = The electrical conductivity

ρ_f = The density of the fluid is the magnetic permeability

D_B = The Brownian diffusion coefficient

D_T = The thermophoretic diffusion

The equations are subjected to the boundary conditions:

$$\begin{aligned}&u=u_w(x)=cx, v=0, H_1=H_2=0, T=T_w,\\&C=C_w \text{ at } y=0\\&u=u_e(x)\to ax, H_1=H_e(x)\to H_0 x, T\to T_\infty,\\&C\to C_\infty \text{ as } y\to\infty\end{aligned} \tag{7}$$

Where:

α and c = Constants with $\alpha>0$ and $\alpha>0$ for stretching sheet and $c<0$ for shrinking sheet

H_0 = The value of the uniform magnetic field at infinity upstream

$u_e(x)$ and $H_e(x)$ = The x-velocity and x-magnetic field at the edge of the boundary layer

Thus, we introduce the following similarity transformations:

$$\psi=(a\nu)^{1/2}xf(x),\ H_1=H_0xh'(\eta),\ H_2=-H_0\left(\frac{\nu}{a}\right)^{1/2}h(\eta),$$
$$\theta(\eta)=\frac{(T-T_\infty)}{(T_w-T_\infty)},\ \varphi(\eta)=\frac{(C-C_\infty)}{(C_w-C_\infty)},\ \eta=\left(\frac{a}{\nu}\right)^{1/2}y \tag{8}$$

where, Ψ is the stream function, which is defined as $u = \partial\Psi/\partial y$ and $v = -\partial\Psi/\partial x$, hence, Eq. 1 and 2 are satisfied. By substituting Eq. 8 into Eq. 3-6, we obtain the following ordinary nonlinear differential equations:

$$f'''+ff''-f'^2+1+M\left(h'^2-hh''-1\right)=0 \tag{9}$$

$$\chi h'''+fh''-f'h=0 \tag{10}$$

$$\frac{1}{Pr}\theta''+f\theta'+Nb\theta'\varphi'+Nt\theta'^2=0 \tag{11}$$

$$\varphi''+Lef\varphi'+\frac{Nt}{Nb}\theta''=0 \tag{12}$$

And the boundary Eq. 7 reduce to:

$$\begin{aligned}&f(0)=0, f'(0)=\lambda, h(0)=0, h'(0)=0, \theta(0)=1,\\&\varphi(0)=1, f'(\infty)=1, h'(\infty)=1, \theta(\infty)=0, \varphi(\infty)=0\end{aligned} \tag{13}$$

Prime denotes differentiation with respect to η:

Where:

Pr = The Prandtl number

M = The magnetic parameter

χ = The reciprocal magnetic Prandtl number

Nb = The Brownian motion parameter
Nt = The thermophoresis parameter
Le = The Lewis number
λ = The stretching ($\lambda>0$) or shrinking parameter ($\lambda<0$)

These parameters are defined as follows:

$$\Pr=\frac{\nu}{\alpha},\ M=\frac{\mu_m H_0^2}{4\pi\rho_f a\nu},\ \chi=\frac{\zeta}{\nu},\ Nb=\frac{\varepsilon D_B(C_w-C_\infty)}{\nu},\ Le=\frac{\nu}{D_B},\ Nt=\frac{\varepsilon D_T(T_w-T_\infty)}{\nu T_\infty},\ \lambda=\frac{c}{a} \quad (14)$$

The quantities of interest are the skin friction coefficient, the local Nusselt number Nu_x and the local Sherwood number Sh_x which defined as:

$$C_f=\frac{\varepsilon_w}{\rho u_e^2},\ Nu_x=\frac{xq_w}{k(T_w-T_\infty)},\ Sh_x=\frac{xq_m}{D_B(C_w-C_\infty)} \quad (15)$$

where the wall skin friction or the shear stress, the wall heat flux q_w and the mass flux q_m are given by:

$$\varepsilon_w=\mu\left(\frac{\partial u}{\partial y}\right)_{y=0},\ q_w=-k\left(\frac{\partial T}{\partial y}\right)_{y=0},\ q_m=-D_B\left(\frac{\partial C}{\partial y}\right)_{y=0} \quad (16)$$

By using nondimensionless variables in Eq. 8, 15 and 16, we obtain:

$$Re_x^{1/2}C_f=f''(0),\ Re_x^{-1/2}Nu_x=-\theta'(0),\ Re_x^{-1/2}Sh_x=-\varphi'(0) \quad (17)$$

where, $Re_x = u_e x/v$ is the Reynolds number.

Stability of solution: In order to perform a stability analysis, the unsteady problem is considered. Equation 1 and 2 hold, while Eq. 3-6 are replaced by:

$$\frac{\partial u}{\partial t}+u\frac{\partial u}{\partial x}+v\frac{\partial u}{\partial y}-\frac{\mu_m}{4\pi\rho_f}\left(H_1\frac{\partial H_1}{\partial x}+H_2\frac{\partial H_2}{\partial y}\right)=\left(u_e\frac{\partial u_e}{\partial x}-\frac{\mu_m H_e}{4\pi\rho_f}\frac{\partial H_e}{\partial x}\right)+\nu\frac{\partial^2 u}{\partial y^2} \quad (18)$$

$$\frac{\partial H_1}{\partial t}+u\frac{\partial H_1}{\partial x}+v\frac{\partial H_1}{\partial y}-H_1\frac{\partial u}{\partial x}-H_2\frac{\partial u}{\partial y}=\zeta\frac{\partial^2 H_1}{\partial y^2} \quad (19)$$

$$\frac{\partial T}{\partial t}+u\frac{\partial T}{\partial x}+v\frac{\partial T}{\partial y}=\alpha\frac{\partial^2 T}{\partial y^2}+\varepsilon D_B\frac{\partial T}{\partial y}\frac{\partial C}{\partial y}+\varepsilon\left(\frac{D_T}{T_\infty}\right)\left(\frac{\partial T}{\partial y}\right)^2 \quad (20)$$

$$\frac{\partial C}{\partial t}+u\frac{\partial C}{\partial x}+v\frac{\partial C}{\partial y}=D_B\frac{\partial^2 C}{\partial y^2}+\left(\frac{D_T}{T_\infty}\right)\frac{\partial^2 T}{\partial y^2} \quad (21)$$

where, t denotes the time. Based on the variables in Eq. 8, we introduce the following new dimensionless variables:

$$u=ax\frac{\partial f}{\partial\eta}(\eta,\tau),\ v=-(a\nu)^{1/2}f(\eta,\tau),\ \eta=(a/\nu)^{1/2}y,\ \tau=at,\ H_1=H_0x\frac{\partial h}{\partial\eta}(\eta,\tau),\ H_2=-(\nu/a)^{1/2}h(\eta,\tau),\ \theta(\eta,\tau)=\frac{(T-T_\infty)}{(T_w-T_\infty)},\ \varphi(\eta,\tau)=\frac{(C-C_\infty)}{(C_w-C_\infty)} \quad (22)$$

So, that Eq. 3-6 can be written as:

$$\frac{\partial^3 f}{\partial\eta^3}+f\frac{\partial^2 f}{\partial\eta^2}-\left(\frac{\partial f}{\partial\eta}\right)^2+1+M\left[\left(\frac{\partial h}{\partial\eta}\right)^2-h\frac{\partial^2 f}{\partial\eta^2}-1\right]-\frac{\partial^2 f}{\partial\eta\partial\tau}=0 \quad (23)$$

$$\chi\frac{\partial^3 h}{\partial\eta^3}+f\frac{\partial^2 h}{\partial\eta^2}-h\frac{\partial^2 f}{\partial\eta^2}-\frac{\partial^2 h}{\partial\eta\partial\tau}=0 \quad (24)$$

$$\frac{1}{\Pr}\frac{\partial^2\theta}{\partial\eta^2}+f\frac{\partial\theta}{\partial\eta}+Nb\frac{\partial\varphi}{\partial\eta}\frac{\partial\theta}{\partial\eta}+Nt\left(\frac{\partial\theta}{\partial\eta}\right)^2-\frac{\partial\theta}{\partial\tau}=0 \quad (25)$$

$$\frac{\partial^2\varphi}{\partial\eta^2}+Lef\frac{\partial\theta}{\partial\eta}+\frac{Nt}{Nb}\frac{\partial^2\theta}{\partial\eta^2}-\frac{\partial\varphi}{\partial\tau}=0 \quad (26)$$

And subject to the new boundary conditions:

$$f(0,\tau)=0,\ f'(0,\tau)=\lambda,\ h(0,\tau)=0,\ h'(0,\tau)=0,\ \theta(0,\tau)=1,\ \varphi(0,\tau)=1,\ f'(\eta,\tau)=1, h'(\eta,\tau)=1,\ \theta(\eta,\tau)=1,\ \varphi(\eta,\tau)=0 \text{ as } \eta\to\infty \quad (27)$$

To test the stability of the steady flow solution:

$$f=f_0(\eta),\ h=h_0(\eta),\ \theta=\theta_0(\eta) \text{ and } \phi=\phi_0(\eta) \quad (28)$$

Satisfying the boundary-value Eq. 1-7, we write:

$$f(\eta,\tau)=f_0(\eta)+e^{-\gamma\tau}F(\eta,\tau),\ h(\eta,\tau)=h_0(\eta)+e^{-\gamma\tau}H(\eta,\tau),\ \theta(\eta,\tau)=\theta_0(\eta)+e^{-\gamma\tau}G(\eta,\tau),\ \varphi(\eta,\tau)=\varphi_0(\eta)+e^{-\gamma\tau}J(\eta,\tau) \quad (29)$$

where, γ is an unknown eigenvalue and $F(\eta, \tau)$, $H(\eta, \tau)$, $G(\eta, \tau)$ and $J(\eta, \tau)$ are small relative to $f_0(\eta)$, $h_0(\eta)$, $\theta_0(\eta)$

and $\phi_0(\eta)$, respectively. Solutions of the eigenvalue problem in Eq. 23-27 give an infinite set of eigenvalues $\gamma_1 < \gamma_2 <, ...,$ If the smallest eigenvalue γ_1 is negative, there is an initial growth of disturbances and the flow is unstable, however, when γ_1 is positive, there is an initial decay and the flow is stable. Introducing Eq. 28 into Eq. 23-27, we get the following linearized problem:

$$\frac{\partial^3 F}{\partial \eta^3}+f_0\frac{\partial^2 F}{\partial \eta^2}+f_0''F-\left(2f_0'-\gamma\right)\frac{\partial F}{\partial \eta}+ M\left[2h_0'\frac{\partial H}{\partial \eta}-h_0\frac{\partial^2 H}{\partial \eta^2}-h_0''H\right]-\frac{\partial^2 F}{\partial \eta\partial \tau}=0 \quad (30)$$

$$\chi\frac{\partial^3 H}{\partial \eta^3}+f_0\frac{\partial^2 H}{\partial \eta^2}-h_0''F-f_0''H-h_0\frac{\partial^2 F}{\partial \eta^2}+ \gamma\frac{\partial H}{\partial \eta}-\frac{\partial^2 H}{\partial \eta\partial \tau}=0 \quad (31)$$

$$\frac{1}{Pr}\frac{\partial^2 G}{\partial \eta^2}+f_0\frac{\partial G}{\partial \eta}+\theta_0'F+Nb\left(\varphi_0'\frac{\partial G}{\partial \eta}+\theta_0'\frac{\partial J}{\partial \eta}\right)+ Nt\left(2\theta_0'\frac{\partial G}{\partial \eta}\right)+\gamma G-\frac{\partial G}{\partial \tau}=0 \quad (32)$$

$$\frac{\partial^2 J}{\partial \eta^2}+Le\left(f_0\frac{\partial J}{\partial \eta}+\varphi_0'F\right)+\frac{Nt}{Nb}\frac{\partial^2 G}{\partial \eta^2}+\gamma J-\frac{\partial J}{\partial \tau}=0 \quad (33)$$

Along with the boundary conditions

$$\begin{aligned}&F(0,\tau)=0,\frac{\partial F}{\partial \eta}(0,\tau)=0,H(0,\tau)=0,\frac{\partial H}{\partial \eta}(0,\tau)=0,\\ &G(0,\tau)=0,\ J(0,\tau)=0,\\ &\frac{\partial F}{\partial \eta}(\eta,\tau)=0,\ \frac{\partial H}{\partial \eta}(\eta,\tau)=0,G(\eta,\tau)=0,\\ &J(\eta,\tau)=0 \text{ as } \eta\to\infty\end{aligned} \quad (34)$$

The solutions $f = f_0(\eta)$, $h = h_0(\eta)$, $\theta = \theta_0(\eta)$ and $\phi = \phi_0(\eta)$ of the steady Eq. 9-13 are obtained by setting $\tau = 0$. Hence, $F(\eta) = F_0(\eta)$, $H(\eta) = H_0(\eta)$, $G(\eta) = G_0(\eta)$ and $J(\eta) = J_0(\eta)$ and in Eq. 29-32 identify initial growth or decay of the solution (Eq. 28). In this respect, we have to solve the linear eigenvalue problem:

$$F_0'''+f_0F_0''+f_0''F_0-\left(2f_0'-\gamma\right)F_0'+ M\left[2h_0'H_0'-h_0H_0''-h_0''H_0\right]=0 \quad (35)$$

$$\chi H_0'''+f_0H_0''+h_0''F_0-f_0''H_0-h_0F_0''+\gamma H_0'=0 \quad (36)$$

$$\frac{1}{Pr}G_0''+f_0G_0'+\theta_0'F_0+Nb\left(\varphi_0'G_0'+\theta_0'J_0'\right)+ 2Nt\theta_0'G_0'+\gamma G_0=0 \quad (37)$$

$$J_0''+Le\left(f_0J_0'+\varphi_0'F_0\right)+\frac{Nt}{Nb}G_0''+\gamma J_0=0 \quad (38)$$

Along with the boundary conditions:

$$\begin{aligned}&F_0(0)=0,\ F_0'(0)=0,\ H_0(0)=0,\ H_0'(0)=0,\ G_0(0)=0,\\ &J_0(0)=0\\ &F_0'(\eta)\to0,\ H_0'(\eta)\to0,\ G_0(\eta)\to0,\ J_0(\eta)\to0 \text{ as } \eta\to\infty\end{aligned} \quad (39)$$

The stability of the steady-state flow solution is based on the smallest eigenvalue, γ_1. Therefore, the condition $F_0'(\eta)\to0$ as $\eta\to\infty$ has been put at rest as suggested by Harris *et al.* (2009) and for a fixed value of eigenvalue, γ. Equation 34-38 are then solved by introducing a new boundary condition that is $F_0''(0)=1$.

RESULTS AND DISCUSSION

The nonlinear ordinary differential Eq. 9-12 with respect to the boundary Eq. 13 are solved numerically using bvp4c solver in MATLAB Software. In this study, for a numerical computation, we have considered the non-dimensional parameter values such as $M = 0.1$, $\chi = 1.0$, $Pr = 6.2$, $Nb = 0.01$, $Nt = 0.01$, $Le = 1.0$ and $\lambda = -1.1$. These values are fixed in the entire study except the varied values as shown in respective figures and tables. In order to validate this present study, we have to make a comparison value of the skin friction coefficient with previous published studies by setting some parameters as shown in Table 1. From Table 2, we obtained a good agreement with the present results. Table 1 also shows non unique solutions (dual solutions) exist when shrinking sheet is considered.

The influence of the non-dimensional parameters such as magnetic parameter M reciprocal magnetic parameter Prandtl number Pr, Brownian motion parameter thermophoresis parameter Lewis number and stretching/shrinking parameter λ on the velocity, magnetic, temperature and concentration profiles are illustrated in Fig. 1-7, respectively. These profiles satisfy the far field boundary Eq. 13, asymptotically which support the validity of the results obtained. From all Fig. 1-7, it can be seen clearly that the boundary layer thickness for lower branch solution always thicker than the upper branch solution. Figure 1-7 also display dual profiles to support the existence of dual solutions.

Table 1: Comparison value of the skin friction coefficient for different values of λ

	Present result		Aman *et al.* (2013)		Bhattacharyya *et al.* in 2013	
λ	Upper branch	Lower branch	Upper branch	Lower branch	Upper branch	Lower branch
-0.25	1.40224		1.4022		1.402240	
-0.3	1.42757		1.4276			
-0.4	1.46861		1.4686			
-0.5	1.49566		1.4957		1.495669	
-0.615	1.50724		1.5072		1.507240	
-0.75	1.48929		1.4893		1.489298	
-1	1.32881	0	1.3288	0	1.328816	0
-1.15	1.08223	0.11670	1.0822	0.1167	1.082231	0.116673
-1.18	1.00044	0.17836	1.0004	0.1784		
-1.2465	0.55429	0.55429	0.5543	0.5543	0.554285	0.554285

Table 2. Smallest eigenvalues γ_1 with various values of λ

λ	First solution (Upper branch)	Second solution (Lower branch)
-1.1	1.1980	-0.6478
-1.15	0.4594	-0.4270
-1.18	0.1346	-0.1316
-1.182	0.0744	-0.0735
-1.1828	0.0235	-0.0234

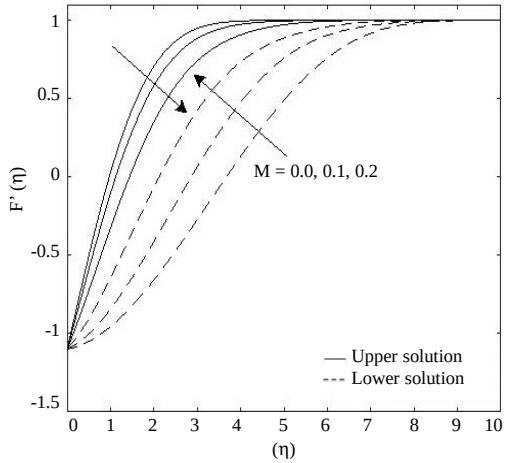

Fig. 1: Velocity profiles for different values of M

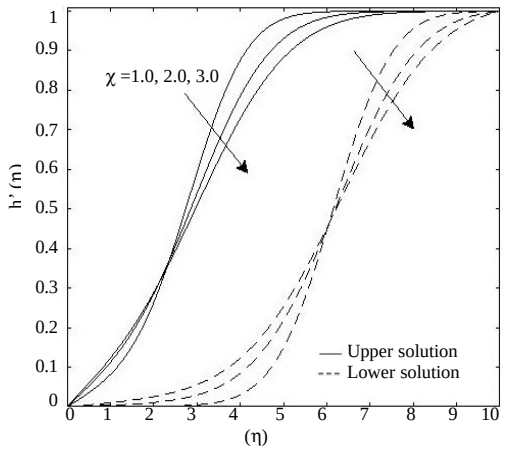

Fig. 2: Magnetic profiles for different values of c

Further, Fig. 8 shows the variation of the skin friction coefficient with the stretching/shrinking λ for various

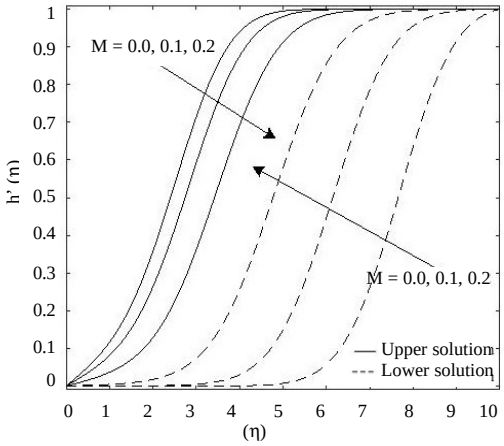

Fig. 3: Magnetic profiles for different values of M

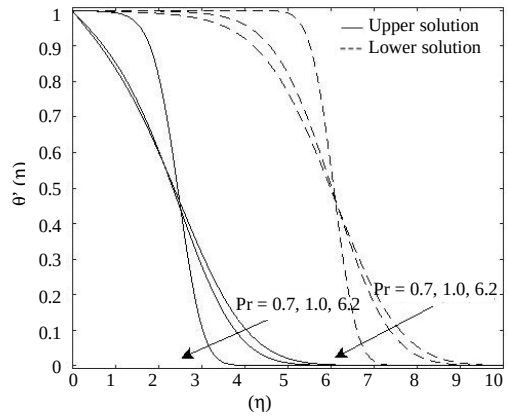

Fig. 4: Temperature profiles for different values of Pr

values of magnetic parameter M. From Fig. 8, it can be observed that the skin friction coefficient decreases as M increases, meaning that the surface shear stress decreases in the present of the magnetic field due to an increment in Lorentz force. Figure 9 indicates the variation of the local Nusselt number with the stretching/shrinking λ for various value of magnetic parameter As the value of increases, the temperature gradient at the surface decreases. Thus, the heat transfer rate at the surface

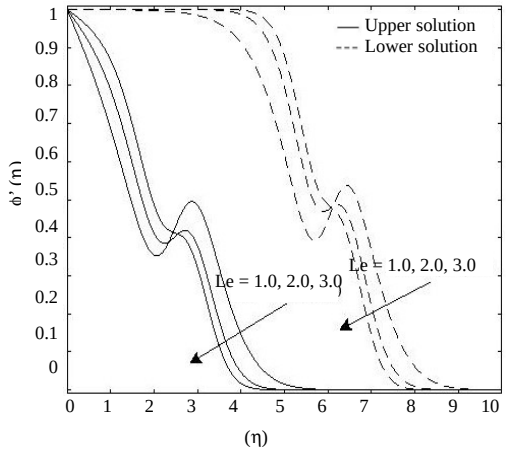

Fig. 5: Concentration profiles for different values of

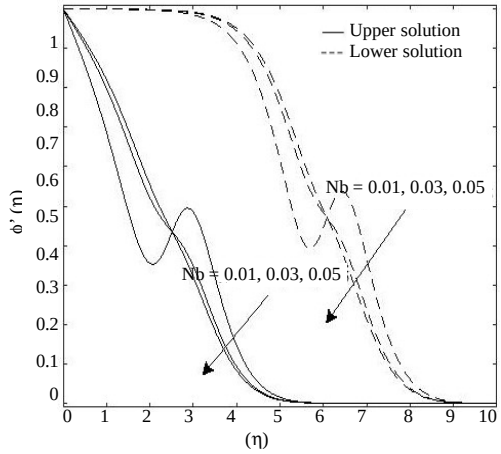

Fig. 6: Concentration profiles for different values of

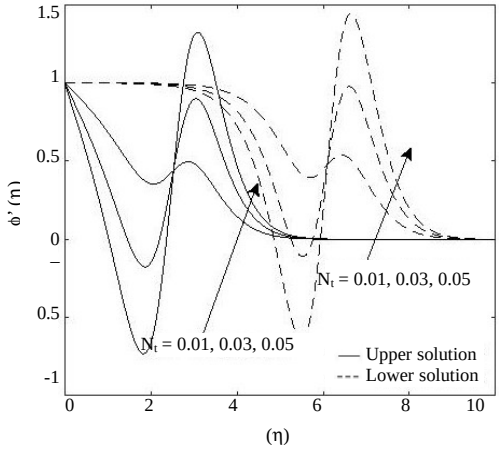

Fig. 7: Concentration profiles for different values of

decreases with the existence of magnetic field. Figure 10 displays the variation of the local Sherwood number with the stretching/shrinking λ for various value of magnetic parameter M. It shows that the mass transfer rate at the

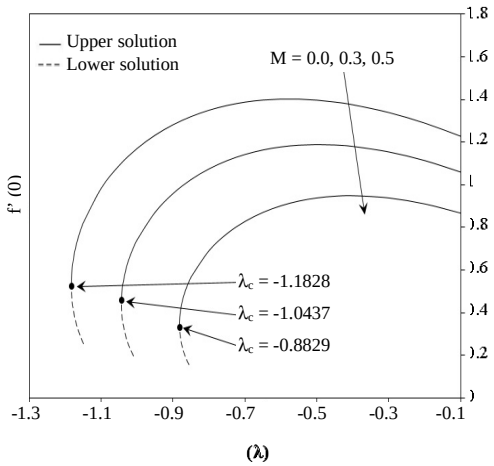

Fig. 8: Variation of the skin friction with l for different values of M

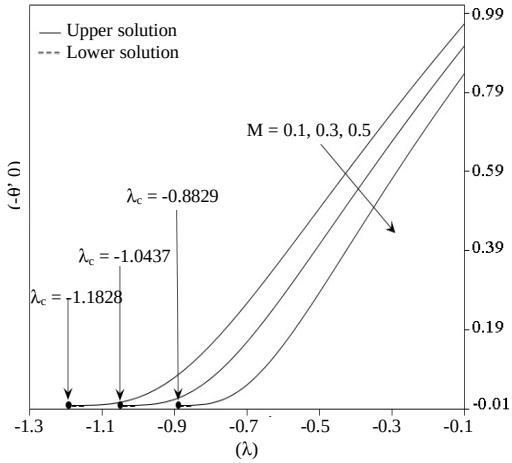

Fig. 9: Variation of the local Nusselt number with l for different values of M

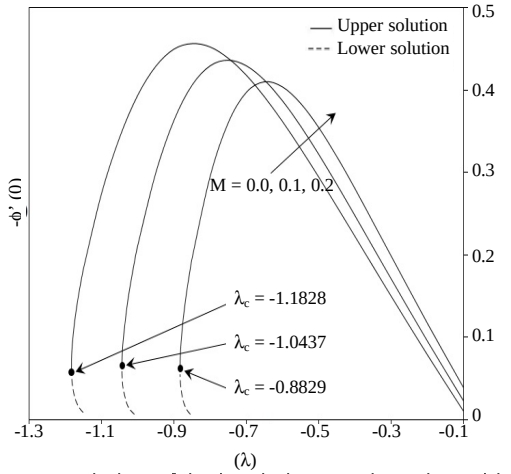

Fig. 10: Variation of the local Sherwood number with l for different values of M

surface decreases as the value of M increases. From Fig. 8-10, dual solutions exist for certain range of λ and

we can figure out that no solution exists beyond certain value where is the critical value and unique solution is obtained when Therefore, the boundary layer separation becomes faster when the magnetic field is applied.

To determine the stability of the dual solutions, we solve the Eigenvalue Eq. 33-37 and find the smallest Eigenvalue Positive value of gives an initial decay and thus the flow is stable while negative value implies the growth of disturbance and the flow is unstable. Table 2 presents the smallest Eigenvalues for selected values of λ. The results indicate that the upper branch solutions have positive smallest eigenvalue while all the lower branch solutions have negative smallest eigenvalue Therefore, the upper branch solution is stable physically while the lower branch is unstable over time.

CONCLUSION

The problem of the steady two dimensional stagnation-point flow of an incompressible electrically conducting nanofluid caused by a stretching/shrinking surface with the effect of induced magnetic field is solved numerically. The existence of dual solutions is clearly shown in the figures. It is also found that the magnetic parameter induces earlier the boundary layer separation from the surface. The stability analysis is performed via. bvp4c function in MATLAB Software to determine which solution is physically stable and it is found that the first solution (upper branch) is stable and valid physically while the second solution (lower branch) is unstable.

ACKNOWLEDGEMENT

The researchers gratefully acknowledge the financial support from IPS grant (Project number: GP-IPS/2018/9570000) from Universiti Putra Malaysia.

REFERENCES

Ali, F.M., R. Nazar, N.M. Arifin and I. Pop, 2011b. MHD boundary layer flow and heat transfer over a stretching sheet with induced magnetic field. Heat Mass Transfer, 47: 155-162.

Ali, F.M., R. Nazar, N.M. Arifin and I. Pop, 2011a. MHD mixed convection boundary layer flow toward a stagnation point on a vertical surface with induced magnetic field. J. Heat Transfer, 133: 1-6.

Ali, F.M., R. Nazar, N.M. Arifin and I. Pop, 2011c. MHD stagnation-point flow and heat transfer towards stretching sheet with induced magnetic field. Appl. Math. Mech., 32: 409-418.

Aman, F., A. Ishak and I. Pop, 2013. Magneto hydrodynamic stagnation-point flow towards a stretching/shrinking sheet with slip effects. Intl. Commun. Heat Mass Transfer, 47: 68-72.

Bachok, N., A. Ishak and I. Pop, 2011. Stagnation-point flow over a stretching/shrinking sheet in a nanofluid. Nanoscale Res. Lett., 6: 623-632.

Buongiorno, J., 2006. Convective transport in nanofluids. ASME J. Heat Transfer, 128: 240-250.

Choi, S.U.S., 1995. Enhancing Thermal Conductivity of Fluids with Nanoparticles. In: Developments and Applications of Non-Newtonian Flows, Siginer, D.A. and H.P. Wang (Eds.). American Society of Mechanical Engineers, New York, pp: 99-105.

Davies, T.V., 1963. The magneto-hydrodynamic boundary layer in the two-dimensional steady flow past a semi-infinite flat plate I, uniform conditions at infinity. Proc. R. Soc. A., 273: 496-508.

Harris, S.D., D.B. Ingham and I. Pop, 2009. Mixed convection boundary-layer flow near the stagnation point on a vertical surface in a porous medium: Brinkman model with slip. Trans. Porous Media, 77: 267-285.

Ishak, A., R. Nazar and I. Pop, 2006. Mixed convection boundary layers in the stagnation-point flow toward a stretching vertical sheet. Meccanica, 41: 509-518.

Kumari, M., H.S. Takhar and G. Nath, 1990. MHD flow and heat transfer over a stretching surface with prescribed wall temperature or heat flux. Warme Stoffubertragung, 25: 331-336.

Kuznetsov, A.V. and D.A. Nield, 2010. Natural convective boundary-layer flow of a nanofluid past a vertical plate. Int. J. Thermal Sci., 49: 243-247.

Makinde, O.D., W.A. Khan and Z.H. Khan, 2013. Buoyancy effects on MHD stagnation point flow and heat transfer of a nanofluid past a convectively heated stretching/shrinking sheet. Intl. J. Heat Mass Transfer, 62: 526-533.

Mansur, S., A. Ishak and I. Pop, 2015. The magnetohydrodynamic stagnation point flow of a nanofluid over a stretching/shrinking sheet with suction. PLoS One, 10: 1-14.

Mustafa, M., T. Hayat, I. Pop, S. Asghar and S. Obaidat, 2011. Stagnation-point flow of a nanofluid towards a stretching sheet. Intl. J. Heat Mass Transfer, 54: 5588-5594.

Nandy, S.K. and T.R. Mahapatra, 2013. Effects of slip and heat generation/absorption on MHD stagnation flow of nanofluid past a stretching/shrinking surface with convective boundary conditions. Intl. J. Heat Mass Transfer, 64: 1091-1100.

Takhar, H.S., M. Kumari and G. Nath, 1993. Unsteady free convection flow under the influence of a magnetic field. Arch. Appl. Mech., 63: 313-321.

Zaimi, K., A. Ishak and I. Pop, 2012. Boundary layer flow and heat transfer past a permeable shrinking sheet in a nanofluid with radiation effect. Adv. Mech. Eng., 4: 1-7.